

Citation for published version:

Yuan, W, Coombs, TA, Kim, JH, Kim, CH, Kvitkovic, J & Pamidi, S 2011, 'Measurements and calculations of transport AC loss in second generation high temperature superconducting pancake coils', *Journal of Applied Physics*, vol. 110, no. 11, 113906. <https://doi.org/10.1063/1.3662174>

DOI:

[10.1063/1.3662174](https://doi.org/10.1063/1.3662174)

Publication date:

2011

[Link to publication](#)

Copyright (2011) American Institute of Physics. This article may be downloaded for personal use only. Any other use requires prior permission of the author and the American Institute of Physics.

The following article appeared in Yuan, W., Coombs, T. A., Kim, J. H., Kim, C. H., Kvitkovic, J. and Pamidi, S., 2011. Measurements and calculations of transport AC loss in second generation high temperature superconducting pancake coils. *Journal of Applied Physics*, 110 (11), 113906, and may be found at <http://dx.doi.org/10.1063/1.3662174>

University of Bath

Alternative formats

If you require this document in an alternative format, please contact:
openaccess@bath.ac.uk

General rights

Copyright and moral rights for the publications made accessible in the public portal are retained by the authors and/or other copyright owners and it is a condition of accessing publications that users recognise and abide by the legal requirements associated with these rights.

Take down policy

If you believe that this document breaches copyright please contact us providing details, and we will remove access to the work immediately and investigate your claim.

Measurements and calculations of transport AC loss in second generation high temperature superconducting pancake coils

Weijia Yuan,^{1,3,a)} T. A. Coombs,¹ Jae-Ho Kim,² Chul Han Kim,² Jozef Kvitkovic,² and Sastry Pamidi²

¹Engineering Department, University of Cambridge, Cambridge CB2 1PZ, United Kingdom

²Center for Advanced Power Systems, 2000 Levy Avenue, Florida State University, Tallahassee, Florida 32310, USA

³Department of Electronic and Electrical Engineering, University of Bath, Bath BA2 7AY, United Kingdom

(Received 17 August 2011; accepted 12 October 2011; published online 2 December 2011)

Theoretical and experimental AC loss data on a superconducting pancake coil wound using second generation (2 G) conductors are presented. An anisotropic critical state model is used to calculate critical current and the AC losses of a superconducting pancake coil. In the coil there are two regions, the critical state region and the subcritical region. The model assumes that in the subcritical region the flux lines are parallel to the tape wide face. AC losses of the superconducting pancake coil are calculated using this model. Both calorimetric and electrical techniques were used to measure AC losses in the coil. The calorimetric method is based on measuring the boil-off rate of liquid nitrogen. The electric method used a compensation circuit to eliminate the inductive component to measure the loss voltage of the coil. The experimental results are consistent with the theoretical calculations thus validating the anisotropic critical state model for loss estimations in the superconducting pancake coil. © 2011 American Institute of Physics. [doi:10.1063/1.3662174]

I. INTRODUCTION

Superconducting pancake coils wound using second-generation (2 G) high-temperature superconductors (HTS) are promising for superconducting electrical power devices, such as superconducting motors, generators, transformers, magnetic energy storage systems, and fault current limiters. Superconducting windings are essential components in these devices. Therefore understanding the electromagnetic behavior as well as calculating the AC losses of superconducting pancake coils are important for predicting the heat load during the operation of superconducting electrical devices. There have been a few papers on calculating the coil AC losses using different techniques such as the finite element method,¹ minimization magnetic energy variation,² and anisotropic critical state model.^{3,4} However, there are few papers comparing the simulation results with the experimental results except Refs. 2 and 5.

This paper is on the use of an anisotropic critical state model to calculate the coil AC losses. This model was originally proposed by Clem *et al.*,³ and was further developed in Refs. 4, 6, and 7. The assumption of this model is that the magnetic flux lines are parallel to the tape wide faces in the subcritical region in the coil.⁴ In the critical region there exists critical current density determined by the magnetic field, while in the subcritical region there exists much smaller current density. Previous papers considered the impact of just the perpendicular magnetic field on the critical current density. In this paper, both the perpendicular and the parallel magnetic field components are considered when the critical current density is calculated.

Substantial efforts have been made over the past 10 years to understand the complex interactions of AC currents and magnetic fields with 2 G materials in simple tapes and cables.^{8,9} There is, however, a need for reliable techniques for AC loss measurement in coils, which is one of the most common form 2 G conductor encounters in electric power devices. Calorimetric techniques offer advantages in versatility in coil size and geometry. However, there are limitations in sensitivity and extensive experimental equipment related to calorimetric measurements. Electromagnetic methods often require relatively simple equipment for measurements on smaller size samples and are fast in response to AC input. Due to the nature of large inductively coupled signals, there are no dependable techniques available for measurement of AC losses in coils and devices with complex magnetic field profiles.

Electrical methods have been widely used for the measurement of short samples which do not impose large inductive signals. The electromagnetic technique used in this study is similar to the one used for short samples, but with extended applicability that involves effectively eliminating large inductively coupled signals.

One of the reasons of studying AC losses in pancake coils of 2 G HTS tape is that there exists a rather large perpendicular magnetic field component to the tape wide face when transport current is passed through the coil. Perpendicular field component affects significantly both the critical current density and AC losses. The electromagnetic properties, particularly AC loss behavior of coils when exposed to significant perpendicular field component needs to be understood to optimize the design of superconducting electric power devices. This paper reports theoretical and experimental results of AC losses in a pancake coil of 2 G conductor made using IBA manufacturing processes.¹⁰

^{a)}Author to whom correspondence should be addressed. Electronic mail: W. Yuan@bath.ac.uk.

II. SIMULATION MODEL

Critical state in superconducting tapes has been solved by Brandt *et al.*,⁸ and an approximation study of critical state in coils using superconducting tapes have been introduced in Ref. 9. The first step to solve the problem is using an approximation that the superconducting region is expanded to the whole thickness of the tapes. When a superconducting pancake coil is carrying a current, we are assuming it has two regions, critical state region and subcritical state region. To simplify the problem, the critical boundaries distinguishing critical and subcritical regions are assumed to be parabola. Since in superconducting pancake coils the superconductors are packed closely together, we have made another assumption that the magnetic flux lines cannot penetrate into the subcritical regions thus they are parallel to the superconductor wide face in the subcritical region, i.e., the perpendicular magnetic field B_z is zero in the subcritical region. Figure 1 presents a picture describing the critical state in the superconducting pancake coil. This picture shows the cross section area of the

coil. The red parabolas represent the critical boundaries, the subcritical region is inside the red parabola, and the critical region is outside the red parabola. The x -axis values of the intersection points of the red parabola and the x -axis, top/bottom surface of the coil are c_1 , c_2 , and c_3 , respectively. a is the half width of the superconducting tape, b is the half height of the superconducting pancake coil.

According to the critical state theory, the critical current density J_c flows in the critical state region of tapes. The critical currents of tapes are affected by both perpendicular and parallel field components, although the perpendicular field has larger impact. In the subcritical region, there is a much smaller current density J_m to guarantee each tape carries the same transport current since the tapes are wound in series into a superconducting pancake coil. On the other hand, the magnetic field in the superconducting pancake coil is determined by the current density in the coil. Therefore if we know the critical boundary, i.e., the parabola, we can solve the equation system (1) below,

$$\begin{cases} x_c = f(B_z) = \begin{cases} J_0 \frac{B_0}{B_0 + \sqrt{B_z(x, z)^2 + k^2 B_z(x, z)^2}}, & \text{where } c(z) < |x| < a \\ \frac{I/D - 2 \int_{c(z)}^a J_c dx}{2c(z)}, & \text{where } |x| < c(z) \end{cases} \\ z = f(J_y) = \sum_x \sum_z B_z(J_y). \end{cases} \quad (1)$$

By solving equation (1) we can get the current density and magnetic field distribution in the superconducting pancake coil, hence we can calculate the perpendicular magnetic field B_z in the subcritical region. If we change the parameters of the critical boundaries, we will get different values of B_z in the subcritical region. Therefore, solving the criti-

cal state problem becomes an optimization process of the critical boundaries which minimizes B_z in subcritical region.

Having solved the critical state in the superconducting pancake coil, we can calculate the AC losses when the coil is carrying a AC transport current. The AC losses in the first quarter starting from a virgin state in the coil would be

$$Q_0 = 2 \int_{-b}^b \int_{c(z)-}^a J_z(x, z) |B_z(x, z)| (a - x) dx dz. \quad (2)$$

The microscopic physical interpretation of this formula is the summation of the energy dissipated by vortices as they move a distance $a-x$ from the edge to their final positions; the force per unit length is $\Phi_0 J_c$, where $\Phi_0 = h/2e$ is the superconducting flux quantum and the density of vortices is $B_z(x, z)/\Phi_0$.³ The macroscopic interpretation of this formula is the integration of the energy density $J \cdot E$, according to Faraday's law, $E = -dB(a-x)/dt$, the integration of E over time will be $B(a-x)$.

There are two ways to calculate the AC losses in a full AC cycle, one way is to calculate critical states at different time steps in a full AC cycle and hence the AC losses, the other way is to only calculate the critical state at the current amplitude in a fully AC cycle and use $4Q_0$ to estimate the AC losses. In Ref. 7 we have demonstrated that the AC losses Q in a full cycle will be close to $4Q_0$, the error of the

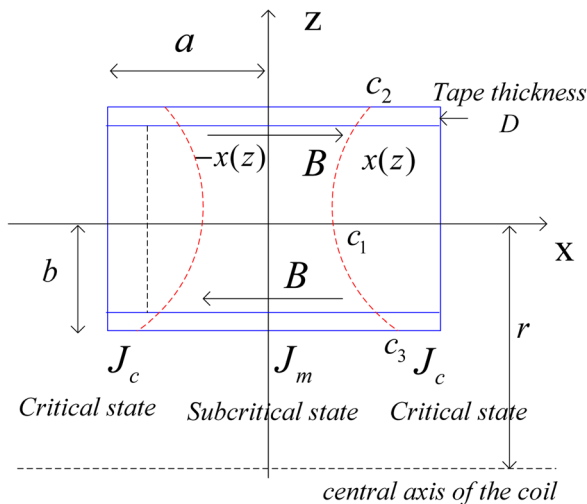


FIG. 1. (Color online) The critical state in the superconducting pancake coil. The critical region is outside the red parabola, and the subcritical region is inside the red parabola.

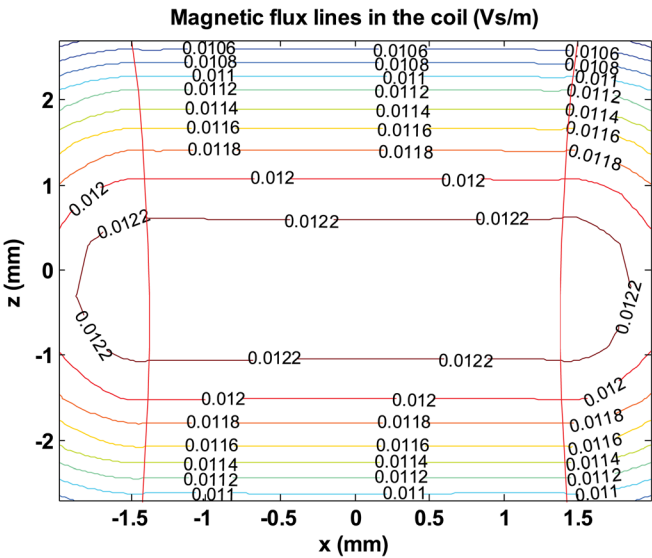


FIG. 2. (Color online) Magnetic flux lines in the coil at 25A.

AC losses by simply using $4Q_0$ compared to calculating critical states in a full cycle is less than 7%, which is acceptable for engineering applications. In addition, using $4Q_0$ only requires us to solve the critical state at the current amplitude in a full AC cycle, which is much faster than solving critical states at different time steps in a full AC cycle.

Figures 2–4 below present a solution example of the critical state of coil a when its transport current is at 25 A. From Fig. 2 we can see that the magnetic flux lines are parallel to the superconducting tapes in the middle subcritical region. The red parabolae represent critical boundaries distinguishing the critical and subcritical regions, while the other color lines represent the magnetic flux lines. Figure 3 show the current density in the coil, and we can find that in the critical region there is a much smaller transport current density. Figure 4 presents the magnetic field distribution in the superconducting pancake coil.

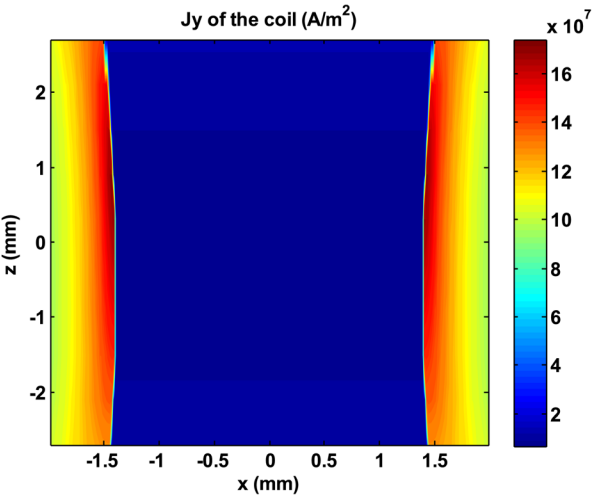


FIG. 3. (Color online) Current density in the coil at 25A.

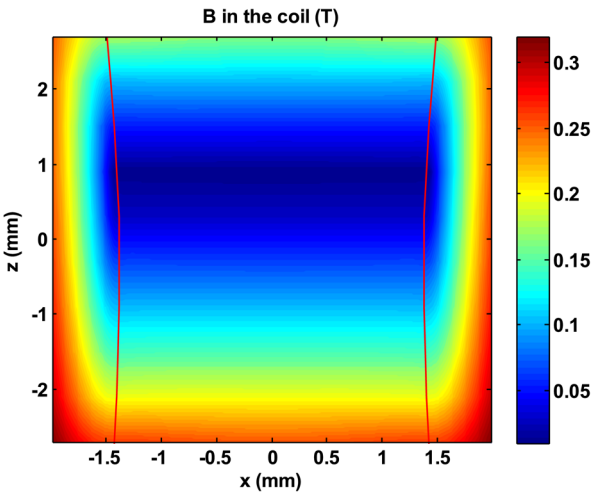


FIG. 4. (Color online) Magnetic field in the coil at 25A.

III. EXPERIMENTAL SETUP FOR AC LOSS MEASUREMENT

A. Coil specification and winding

Table I summarizes the specifications of the pancake coil fabricated. The coil was wound using insulated tape by GE varnish. The conductor was purchased from SuperPower Inc. that uses the ion beam assisted deposition (IBAD) process¹⁰ and has 40 turns.

B. Calorimetric method

Transport AC loss in the coil was measured in boil-off chamber as seen in Fig. 5. The liquid nitrogen boil-off measurement technique is based on enclosing the HTS coil in a sealed fiber glass reinforced epoxy experimental chamber filled with liquid nitrogen. The heat caused by the AC losses boils the corresponding amount of liquid nitrogen. The evaporated nitrogen gas comes out of the chamber through stainless steel outlet tubes to the flow meters. The gas is at the room temperature before it reaches the flow meters. The rate of gas evolution is measured using calibrated nitrogen gas flow meters in standard liters per minute (SLPM). The measured nitrogen gas flow rate can be used to directly infer the extent of AC losses. To minimize the heat leak from

TABLE I. Parameters of the superconducting pancake coil.

Coil parameters	Value
Tape maker	Superpower
Turns	40
Wire width (mm)	4
Wire thickness (mm)	0.15
Length (m)	7.49
Coil I_c (A)@77K	38
Tape I_c (A) @77K, self field	102
ID (mm)	57
OD (mm)	69
Experiments done	
I_{rms} range (A)	10–24
Frequency range (Hz)	100–800

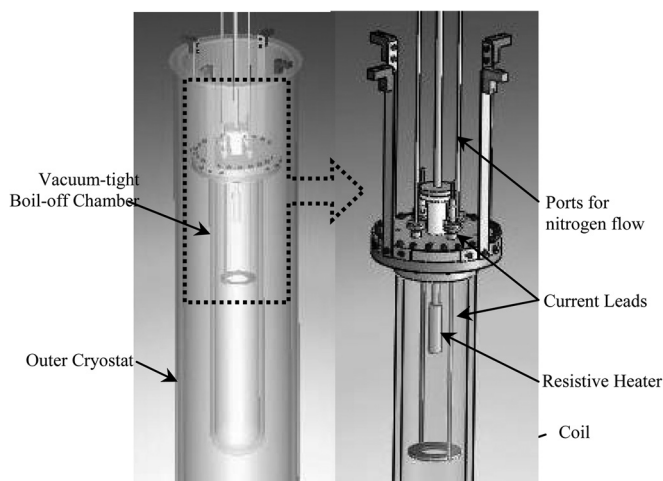


FIG. 5. Schematic of the experimental apparatus used for AC loss measurements in superconducting pancake coils using calorimetric liquid nitrogen boil-off technique.

outside, the experimental chamber is immersed in liquid nitrogen contained in an external dewar. The liquid nitrogen in the external container intercepts heat from the current leads in addition to maintaining zero temperature gradient between the inside and outside of the experimental chamber.

The external nonmagnetic stainless steel cryostat (dewar flask) is 181 cm in height and 31 cm in inner diameter. The experimental calorimetric chamber is 91 cm in length and 14 cm in inner diameter. It has a stainless steel ConFlat flange and hangs inside the outer cryostat concentrically. The top flange of the experimental chamber was sealed with copper gasket creating a cryogenic and vacuum tight seal when the experimental chamber is immersed in liquid nitrogen in the outer cryostat during experiments. For large flow rates, two flow meters were used in parallel to prevent pressure buildup in the chamber.

A resistive heater in the experimental chamber was used to confirm the accuracy and linearity of the liquid nitrogen boil-off measurement setup. Calibration was performed using a heater with 13 Ω resistance and a constant current source. The system was tested for accuracy up to 130 W of input power. The slope of flow rate versus heat input plot, as

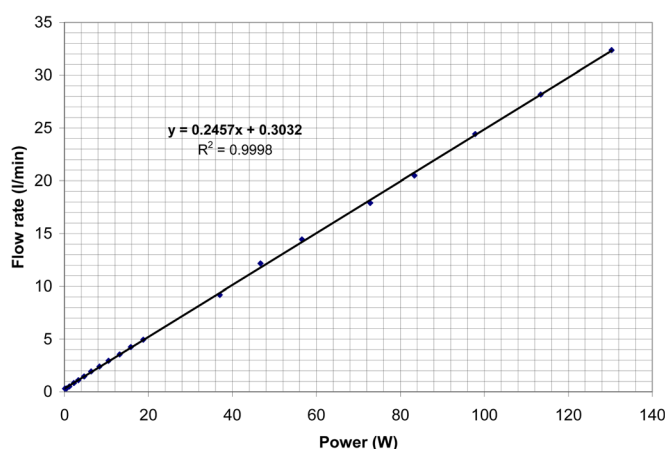


FIG. 6. (Color online) Calibration of nitrogen boil-off method by resistive heater, relation between heater power and nitrogen gas flow rate.

depicted in Fig. 6 was found to be 0.2457 SLPM/W, agreeing well with the theoretical value of 0.25 SLPM/W.⁹

C. Electrical method

The pancake coil was supplied with an AC current using a power amplifier controlled by a function generator. The voltage loss signal from potential taps between the ends of the coil is superposed with very high inductive component that can be eliminated using cancellation coil by eliminating any phase difference between the source current and the measured voltage signal. The Lussajous curve pattern was used to indicate the phase difference between two sine waves of the same frequency for fine compensation of the inductive component.

Figure 7 shows the circuit diagram of the transport AC loss measurement by the electrical method with high accuracy data acquisition (DAQ) system. Only the resistive component of the voltage across the coil represents the ac loss. The signal from the tunable cancellation coil was connected in anti-series with the signal from the voltage taps of the superconducting pancake coil to compensate the inductive component. The cancellation voltage was adjusted to minimize the phase difference between the input current (to the coil) and the voltage signal sum from the superconducting pancake and cancellation coil combination. The cancellation wire is using very thin wires to eliminate eddy current losses. Therefore the resulting voltage represents only the resistive component and hence was recorded as the loss voltage.

The voltage signal of the pancake coil was amplified by an isolation amplifier and passed through a band-pass filter in order to enhance the signal-to-noise ratio and remove the harmonic components using a high accuracy DAQ measurement system with the LabVIEW program. The transport AC loss of the pancake coil per cycle is given as

$$Q_t = I_{rms} V_{rms} / f, \quad (3)$$

where f is frequency, I_{rms} and V_{rms} are in-phase current and voltage, respectively.

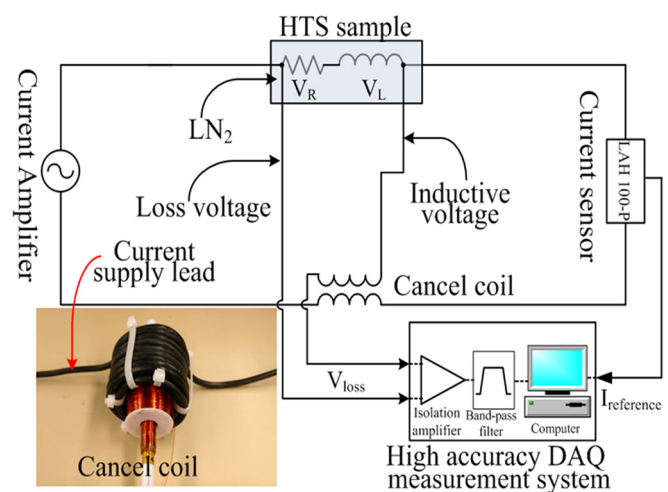


FIG. 7. (Color online) Circuit diagram of electrical method showing the cancellation coil used to eliminate the inductive component for AC loss measurement.

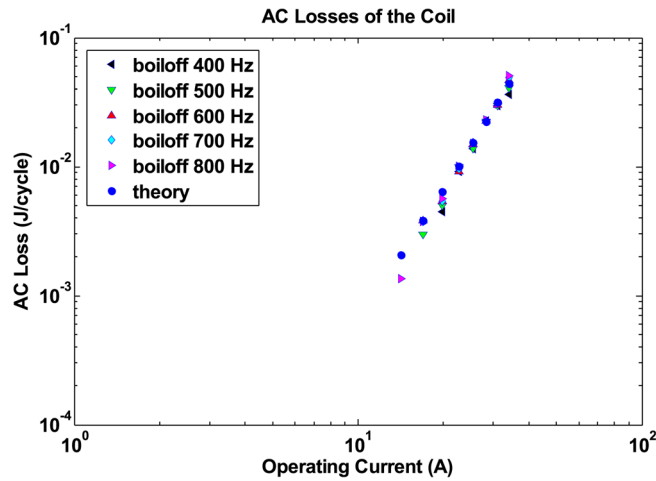


FIG. 8. (Color online) Comparison of simulation results of coil AC losses with that of experimental using calorimetric measurements.

IV. COMPARISON OF SIMULATION AND EXPERIMENTAL RESULTS

Figures 8 and 9 present the comparison between the experimental results and the theoretical calculations. We could find that the results are generally consistent. Figure 8 gives the comparison between the calorimetric measurement results and the theoretical calculations. The results are consistent in the full experiment range. Figure 9 presents the comparison between the electric measurement results and the theoretical calculations. We can find from Fig. 9 that there is a discrepancy between the theoretical and experimental results at large currents. This is mainly coming from the modeling work. From Eq. (1), we can accurately calculate I_c using the data in Table II when the field is not large. However, I_c will be underestimated when the field is large, hence results in an overestimate of AC losses at large currents. The discrepancy at small currents is mainly coming from the electrical measurement results at high frequencies. The electrical measurement results are larger than the calcu-

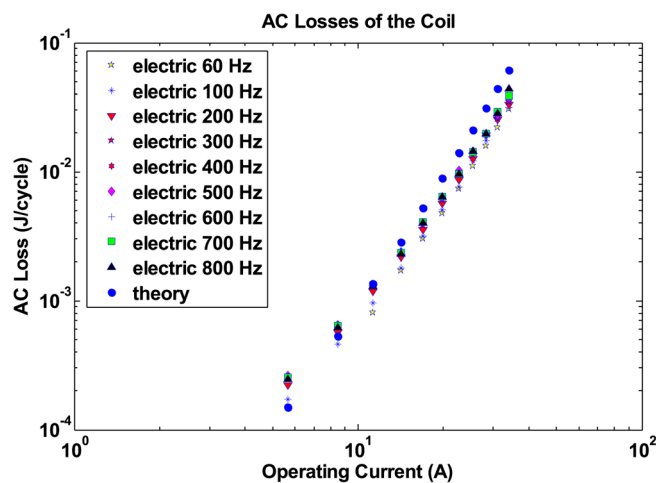


FIG. 9. (Color online) Comparison of simulation results of coil AC losses with that of experimental using electrical method.

TABLE II. Parameters for equation (1).

Parameters	Value
a	2 mm
D	0.15 mm
J_0	1.79×10^8 A/mm ²
B_0	0.047 T
K	0.44

lation because there is a relatively large eddy current loss, although we can find that the calculation is consistent with the measurements at low frequencies.

V. SUMMARY AND DISCUSSIONS

This paper presents an anisotropic critical model for 2 G superconducting pancakes carrying AC transport currents. In the critical region of the coil there is a critical current density, while in the subcritical region there is a much smaller transport current density which guarantees each tapes carries the same transport current. This model assumes in the subcritical region of the coil the magnetic flux lines are parallel to superconducting tapes. By using this model we can solve the critical state in 2 G superconducting pancake coils.

To validate this model, experimental set-ups have been built to measure the transport AC losses in the superconducting pancake coils. Two different methods, electric and calorimetric method, were used in the experiments. The experimental results are consistent with the model calculations and hence validate the anisotropic critical state model.

We have to point out that this model might not be applicable to the coils made of superconducting tape with a ferromagnetic substrate, since it only considers the losses in the superconducting layer. Further modifications will be applied to this model to take into account the ferromagnetic substrate of 2 G superconducting tape.

ACKNOWLEDGMENTS

The authors acknowledge funding from Office of Naval Research through the Center for Advanced Power Systems. The authors would also like to acknowledge Professor Campbell for his help in the modeling work.

¹R. Brambilla, F. Grilli, D. N. Nguyen, L. Martini, and F. Sirois, *Supercond. Sci. Technol.* **22**, 075018 (2009).

²J. Souc, E. Pardo, M. Vojenciak, and F. Gomory, *Supercond. Sci. Technol.* **22**, 015006 (2009).

³J. R. Clem, J. H. Claassen, and Y. Mawatari, *Supercond. Sci. Technol.* **20**, 1130 (2007).

⁴Weijia Yuan, A. M. Campbell, and T. A. Coombs, *Supercond. Sci. Technol.* **22**, 075028 (2009).

⁵F. Grilli and S. P. Ashworth, *Supercond. Sci. Technol.* **20**, 794 (2007).

⁶Weijia Yuan, A. M. Campbell, and T. A. Coombs, *J. Appl. Phys.* **107**, 093909 (2010).

⁷Weijia Yuan, A. M. Campbell, Z. Hong, M. D. Ainslie, and T. A. Coombs, *Supercond. Sci. Technol.* **23**, 085011 (2010).

⁸E. H. Brandt and M. Indenbom, *Phys. Rev. B* **48**, 893 (1993).

⁹H. Okamoto, *IEEE Trans. Appl. Supercond.* **16**, 2 (2006).

¹⁰www.superpower.com For information about IBAD process.